Discretization of the sub-Riemannian Heisenberg Group

Evgeny G. Malkovich[1*]

[1]*Novosibirsk State University and Sobolev Institute of Mathematics, Russia*

[*] e.malkovich@g.nsu.ru, malkovich@math.nsc.ru

ABSTRACT. In this article, we present a discrete model of the sub-Riemannian Heisenberg group $\mathcal{H}$, which serves as an analog of a triangulation of a two-dimensional surface embedded in $\mathbb{R}^3$. The constructed discrete model is represented by a spatial graph Γ_r with weighted edges. The shortest paths within Γ_r approximate geodesics in $\mathcal{H}$.

Keywords: Nonholonomic distribution, Heisenberg group, discrete geometry, computational geometry, sub-Riemannian spheres, geodesics, shortest paths in a graph, tortuosity.

1. INTRODUCTION

The Heisenberg group $\mathcal{H}$ is one of the best known and straightforward examples of nonholonomic geometry. It consists of the three-dimensional space $\mathbb{R}^3$ equipped with a two-dimensional non-integrable subbundle of the tangent bundle $T\mathbb{R}^3$. In the context of the Heisenberg group, the planes Π of admissible directions are spanned by two vector fields, X and Y:

$$X = \frac{\partial}{\partial x} - \frac{y}{2}\frac{\partial}{\partial z}, \; Y = \frac{\partial}{\partial y} + \frac{x}{2}\frac{\partial}{\partial z}. \tag{1}$$

It is straightforward to verify that the Lie bracket $[X, Y] = \frac{\partial}{\partial z}$. According to Frobenius theorem, there is no foliation of $\mathbb{R}^3$ into a family of two-dimensional surfaces Σ such that X and Y are tangent to Σ; this is equivalent to the non-integrability of distribution. In this scenario, it is quite clear that the normal vector $\overrightarrow{n}$ of the plane Π would need to be the gradient of some function $F = F(x, y, z)$ up to multiplication by a scalar function $\lambda = \lambda(x, y, z)$:

$$\lambda\overrightarrow{n} = \lambda X \times Y = \lambda(\frac{y}{2}, -\frac{x}{2}, 1) = (F'_x, F'_y, F'_z).$$

It is not hard to check that there are no solutions $\lambda(x, y, z)$ and $F(x, y, z)$ of this system of PDEs: from the first two equations it easy to show that F should be a function depending only on $\phi = \arctan\frac{y}{x}$ and z; usind the third equation one will find that F doesn't depend on ϕ either; after that it is

clear that there are no non-trivial solutiouns. In contrast, in the integrable (or holonomic) case the family of surfaces Σ is defined as the level sets of some function F

$$\Sigma = \{p \in \mathbb{R}^3 | F(p) = \text{const}\}.$$

To discretize a smooth surface Σ, one can simply define a triangulation of this surface. If the triangles in this triangulation are sufficiently small, they can approximate the pieces of the surface accurately.

For the non-holonomic geometry on $\mathcal{H}$, we can consider a small disk $D_\varepsilon = \{\alpha X + \beta Y | \alpha^2 + \beta^2 < \varepsilon^2\} \subset \Pi$ as a "two-dimensional piece of the Heisenberg group" [1]. However, it turns out that a discrete model of the Heisenberg group, represented as a set of intersecting disks, fails to capture the essential geometric features of $\mathcal{H}$.

To construct a viable discrete model of $\mathcal{H}$, we define a local sub-Riemannian distance between sufficiently close points. This distance is generated by the distribution (1), similar to how it is approached in Heron's problem. Subsequently, we define a spatial graph Γ_r as a discretization of the sub-Riemannian Heisenberg group. Numerical experiments indicate that the metric properties of this graph — such as the shape of the shortest paths — effectively simulate the corresponding properties of the Heisenberg group.

There is a series of works [2, 3, 4] that explore discrete non-holonomic systems from the perspectives of finite-difference operators and computational methods. For instance, in the article titled "On Discrete Geometry of Non-Holonomic Spaces" [5], the authors examine a discrete version of the Lagrange-d'Alembert-Chaplygin equations without delving into specific discrete geometric objects. This work aims to construct a tangible discrete model for $\mathcal{H}$ — the simplest example of sub-Riemannian geometry.

2. LOCAL SUB-RIEMANNIAN DISTANCE

Consider two arbitrary points $p_i = (x_i, y_i, z_i)$ and $p_j = (x_j, y_j, z_j)$ in $\mathcal{H}$. Each point defines a plane spanned by the vectors $X_i = (1, 0, -\frac{y_i}{2})$ and $Y_i = (0, 1, \frac{x_i}{2})$. A normal vector to this plane is given by $N_i = (\frac{y_i}{2}, -\frac{x_i}{2}, 1)$. The corresponding planes are:

$$\Pi_i : \frac{y_i}{2}(x - x_i) - \frac{x_i}{2}(y - y_i) + (z - z_i) = 0$$

$$\Pi_j : \frac{y_j}{2}(x - x_j) - \frac{x_j}{2}(y - y_j) + (z - z_j) = 0.$$

The intersection of these planes defines a line $l_{ij} = \Pi_i \bigcap \Pi_j$, which can be expressed in parametric form:

$$l_{ij}(t) = \begin{pmatrix} \frac{(z_j - z_i)(x_i + x_j)}{x_i y_j - x_j y_i} \\ \frac{(z_j - z_i)(y_i + y_j)}{x_i y_j - x_j y_i} \\ \frac{z_i + z_j}{2} \end{pmatrix} + t \begin{pmatrix} 2x_j - 2x_i \\ 2y_j - 2y_i \\ x_i y_j - x_j y_i \end{pmatrix}.$$

We define the *local sub-Riemannian (lsR) distance* between the two points p_i and p_j as the length of the shortest broken line consisting of two segments that connect these points within the union of the two planes $\Pi_i \bigcup \Pi_j$.

$$\mathbf{d}_{\mathrm{lsR}}(p_i, p_j) = \min_{q \in l_{ij}}(\rho(p_i, q) + \rho(q, p_j)),$$

where ρ is the standard Euclidean distance in $\mathbb{R}^3$. This approach generalizes the classic Heron's problem of finding a point q on a fixed line that minimizes the sum of distances to two fixed points. One of the planes, let's say Π_i, can be rotate about the line l_{ij} until it coincides with the another plane Π_j and the points p_i and p_j will be placed in the different half-planes defined by the line l_{ij}. Then

$$\mathbf{d}_{\mathrm{lsR}}(p_i, p_j)^2 = \rho(p_i', p_j)^2 = (\rho_i + \rho_j)^2 + (\rho(p_i^\perp, p_j^\perp))^2, \qquad (2)$$

as can be seen in the Fig.1. Here $p_i^\perp$ is the projection of p_i onto l_{ij} and $\rho_i = \rho(p_i, p_i^\perp)$.
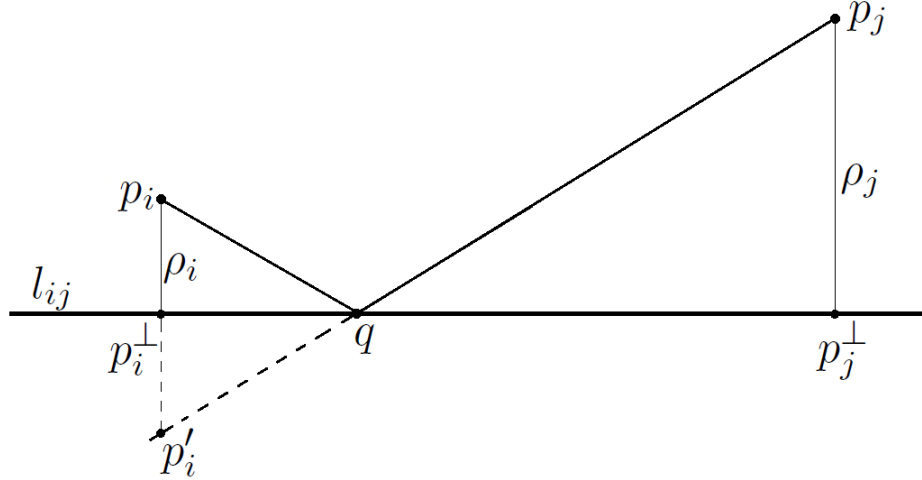

FIGURE 1. The local sub-Riemannian distance $\mathbf{d}_{\mathrm{lsR}}(p_i, p_j)$ and Heron's problem.

The distances ρ_i and ρ_j can be calculated easily

$$\rho_i = \frac{|x_i y_j - x_j y_i + 2z_i - 2z_j|}{\sqrt{4(x_i - x_j)^2 + 4(y_i - y_j)^2 + (x_i y_j - x_j y_i)^2}}\sqrt{4 + x_i^2 + y_i^2}, \qquad (3)$$

$$\rho_j = \frac{|x_i y_j - x_j y_i + 2z_i - 2z_j|}{\sqrt{4(x_i - x_j)^2 + 4(y_i - y_j)^2 + (x_i y_j - x_j y_i)^2}}\sqrt{4 + x_j^2 + y_j^2}. \qquad (4)$$

The distance $\rho(p_i^{\perp}, p_j^{\perp})$ between the projections of the points on the line l_{ij} is

$$\rho(p_i^{\perp}, p_j^{\perp})^2 = \frac{\left(2(x_i - x_j)^2 + 2(y_i - y_j)^2 + (z_j - z_i)(x_i y_j - x_j y_i)\right)^2}{4(x_i - x_j)^2 + 4(y_i - y_j)^2 + (x_i y_j - x_j y_i)^2}. \quad (5)$$

Gathering $(3) - (5)$ and substituting them into (2) gives the lsR-distance:

$$\mathbf{d}_{\mathrm{lsR}}(p_i, p_j) = \frac{1}{\sqrt{4(x_i - x_j)^2 + 4(y_i - y_j)^2 + (x_i y_j - x_j y_i)^2}} \cdot$$

$$\cdot \left((x_i y_j - x_j y_i + 2z_i - 2z_j)^2 \left(\sqrt{4 + x_i^2 + y_i^2} + \sqrt{4 + x_j^2 + y_j^2} \right)^2 + \quad (6) \right.$$

$$\left. + \left(2(x_i - x_j)^2 + 2(y_i - y_j)^2 + (z_j - z_i)(x_i y_j - x_j y_i) \right)^2 \right)^{\frac{1}{2}}.$$

We will use formula (6) to define weights of the edges in a graph Γ_r. Next we set p_1 as an origin point $O \in \mathcal{H}$ and examine the ball $B(O, 1)$ with respect to the lsR-distance.

$$\mathbf{d}_{\mathrm{lsR}}(O, (x, y, z)) = \sqrt{x^2 + y^2} \cdot \sqrt{1 + \frac{z^2}{(x^2 + y^2)^2}(2 + \sqrt{4 + x^2 + y^2})^2}. \quad (7)$$

It is evident that the vertical axis Oz is 'forbidden' — points p_i and p_j having different z coordinate define parallel planes Π_i and Π_j. Consequently, the lsR-distance $\mathbf{d}_{\mathrm{lsR}}(O, (0, 0, z))$ becomes infinite (as illustrated in Fig. 2). This contrasts with the standard sub-Riemannian ball in the Heisenberg group, which takes on an 'apple' shape [6, 7]. In contrast, the lsR-distance results in a pinched ball resembling a donut with an infinitely small hole.
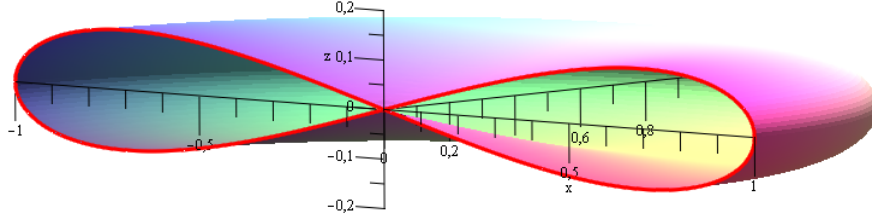

FIGURE 2. The hemisphere in the $\mathbf{d}_{\mathrm{lsR}}$-distance and its ∞-shaped Oxz-section (red).

The sub-Riemannian distance $\mathbf{d}_{\mathrm{sR}}$ from the origin O to the point (x, y, z) in the Heisenberg group $\mathcal{H}$ is defined as follows [7]:

a) if $z = 0$, then $\mathbf{d}_{\mathrm{sR}}(O, (x, y, 0)) = \sqrt{x^2 + y^2}$,

b) if $z \neq 0$ and $x = y = 0$, then $\mathbf{d}_{\mathrm{sR}}(O, (0, 0, z)) = \sqrt{2\pi|z|}$,

c) if $z \neq 0$ and $x^2 + y^2 > 0$, then $\mathbf{d}_{\mathrm{sR}}(O, (x, y, z)) = \frac{q}{\sin q}\sqrt{x^2 + y^2}$,

where

$$\frac{2q - \sin 2q}{4\sin^2 q} = \frac{z}{x^2 + y^2}. \quad (8)$$

The Taylor expansion of (7) gives

$$\mathbf{d}_{\mathrm{lsR}}(O,(x,y,z)) = \sqrt{x^2+y^2}\Big(1 + \frac{1}{2}\frac{z^2}{(x^2+y^2)^2}(2+\sqrt{4+x^2+y^2})^2 + ...\Big).$$

In the general case **c)** of the sub-Riemannian distance, assuming that q is small enough, from (8) one gets

$$q \sim \frac{3z}{x^2+y^2}.$$

Then

$$\mathbf{d}_{\mathrm{sR}}(O,(x,y,z)) = \sqrt{x^2+y^2}\Big(1 + \frac{1}{2}\frac{3z^2}{(x^2+y^2)^2} + ...\Big).$$

The second term in this expansion can be interpreted as a sub-Riemannian correction to the 2-dimensional Euclidean distance function $\sqrt{x^2+y^2}$. Notably, both corrections share a common multiplier of the form $\frac{3z^2}{(x^2+y^2)^2}$, which is a positive indication. It is possible to introduce an additional parameter Λ into the *lsR*-distance (7) that changes the weight of the $(\rho(p_i^\perp, p_j^\perp))^2$ summand, namely

$$\sqrt{x^2+y^2} \cdot \sqrt{1 + \Lambda\frac{z^2}{(x^2+y^2)^2}(2+\sqrt{4+x^2+y^2})^2}.$$

As Λ approaches zero, the ball $B(O,1)$ becomes thicker; conversely, as $\Lambda \to \infty$, it flattens out — transforming from a donut to a pancake: $B(O,1) \to D_1$. It is crucial to note that if the *lsR*-ball $B(O,1)$ were merely a 2-dimensional disc D_1, then the distance between almost any pair of random points would be infinite.

If the center of the ball shifts from the origin to the point p_i, the ball bends in such a way that its central plane of symmetry coincides with the plane Π_i of admissible directions at p_i (Fig.3).

3. A spatial graph and a discrete sub-Riemannian distance

Consider the cubic domain $\Omega = [-1,1]^3 \subset \mathcal{H}$ with a set $D = \{p_i \in \Omega | i = 1, \ldots, N\}$ of N points. These points can form either a regular lattice or they can be randomly and uniformly distributed in Ω. We will consider the scenario with random points. Calculate all distances $\mathbf{d}_{\mathrm{lsR}}(p_i, p_j)$ using (6) and consider the weighted spatial graph Γ_r with vertices p_i and edges v_{ij} of weight $\mathbf{d}_{\mathrm{lsR}}(p_i, p_j) \leq r$, it means that vertices $p_i \in D$ and p_j are connected by the edge v_{ij} in the graph Γ_r if and only if the local sub-Riemannian distance $\mathbf{d}_{\mathrm{lsR}}(p_i, p_j)$ between them is smaller than a fixed value r.

The graph Γ_r serves as a discrete model for the Heisenberg group. When the parameter r is too small, most vertices in Γ_r tend to be disjoint. Conversely, if r is excessively large, nearly all pairs of points (p_i, p_j) will be connected by an edge. The critical threshold value r^* is influenced by both the number of vertices N and the domain Ω. Here, r^* refers to the specific
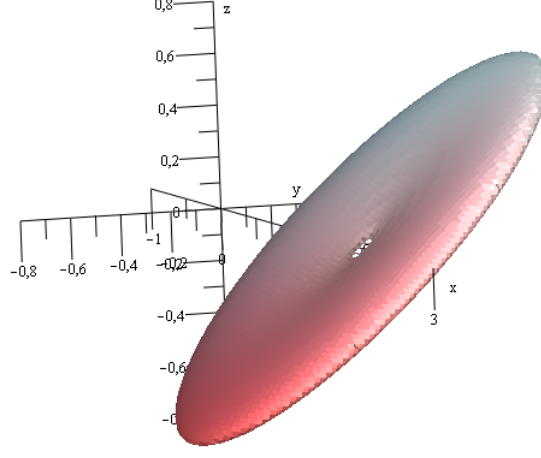
FIGURE 3. The ball $B((2, 0, 0), 1)$ in the $\mathbf{d}_{\text{lsR}}$-distance.

value of r such that for any $r > r^*$, the graph Γ_r becomes connected for an average distribution of the points p_i.

Next we perform a number of numerical experiments demonstrating that the presented discrete model possesses features specific for the sub-Riemannian Heisenberg group. Firstly, using the standard Dijkstra algorithm [8] for finding shortest paths in a graph, one can find the shortest path in Γ_r. The shortest path is a broken line with vertices at the points $p_1, p_{i_1}, \ldots, p_{i_k}, p_2$, thus the *discrete sub-Riemannian (dsR) distance* between p_1 and p_2 in Γ_r is

$$\mathbf{d}_{\text{dsR}}(p_1, p_2) = \mathbf{d}_{\text{lsR}}(p_1, p_{i_1}) + \mathbf{d}_{\text{lsR}}(p_{i_1}, p_{i_2}) + \ldots + \mathbf{d}_{\text{lsR}}(p_{i_k}, p_2). \quad (9)$$

The distance between close vertices is defined via the local sub-Riemannian distance, while the distance between arbitrary vertices is the length of the shortest path in Γ_r.

Numerical calculations show that the shortest path between $p_1 = (0, 0, 0)$ and $p_2 = (0, 0, z_2)$ has a form of a single-wind helix (Fig.4) — a typical form for the Heisenberg geodesics [7, 9]:

$$x(t) = (\sin(\theta_0 + h_3 t) - \sin \theta_0)/h_3,$$

$$y(t) = (\cos \theta_0 - \cos(\theta_0 + h_3 t))/h_3, \quad (10)$$

$$z(t) = (h_3 t - \sin h_3 t)/h_3^2.$$

In (10) the parameter θ_0 can be chosen in such a way that the initial velocity vector at $t = 0$ coincides with the first interval $[p_1, p_{i_1}]$ and the varying parameter h_3 gives the necessary height $z(2\pi)$ of the helix (Fig.4, black curve). Note that the discrete sub-Riemannian distance between points having different z coordinate is finite, contrary to the local sub-Riemannian distance.
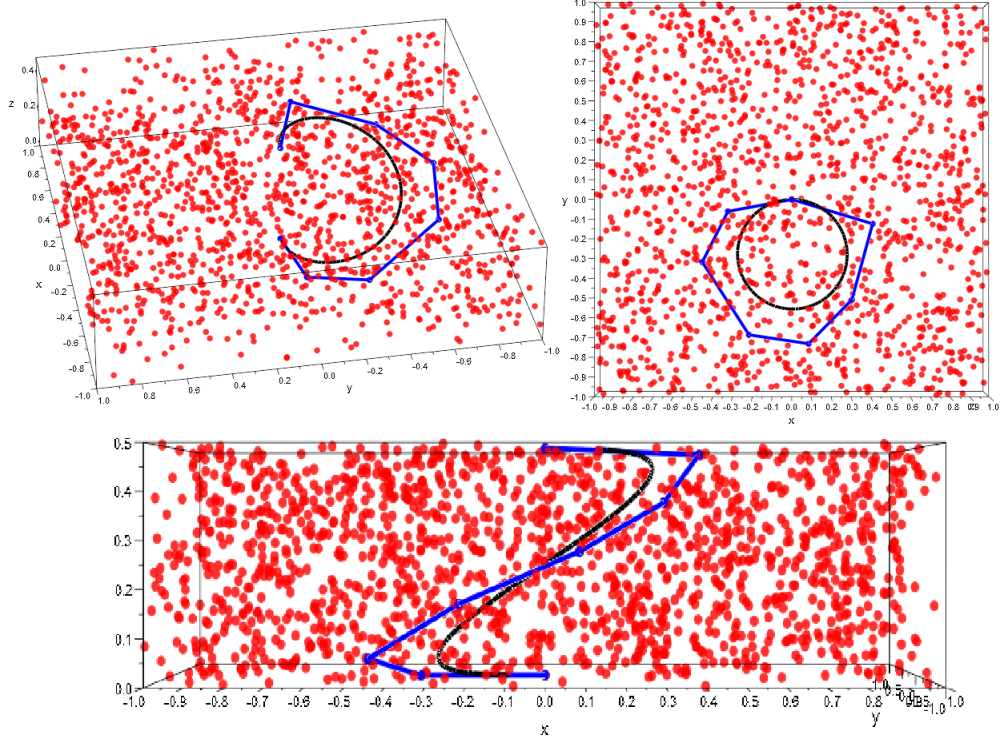
FIGURE 4. Sub-Riemannian geodesic (black, (10)) and typical shortest path (blue) in the graph $\Gamma_{\frac{1}{2}}$ with $N = 1500$ vertices connecting points $(0,0,0)$ and $(0,0,\frac{1}{2})$, various projections.

Next we compare the distance $\mathbf{d}_{\mathrm{dsR}}$ between points as the vertices of the graph Γ_r and the sub-Riemannian distance $\mathbf{d}_{\mathrm{sR}}$ in $\mathcal{H}$. We will consider two situations: horizontal and vertical. In the horizontal case, when $p_1 = (0,0,0)$ and $p_2 = (x_2, y_2, 0)$, the geodesic in $\mathcal{H}$ is a straight horizontal interval $[p_1, p_2]$ in the plane Oxy. The vertical situation is when $p_1 = (0,0,0)$ and $p_2 = (0,0,z_2)$ and the geodesic is a helix (10) with non-constant slope. In accordance with **a**) the sub-Riemannian distance in the horizontal case coincides with the Euclidean length $\mathbf{d}_{sR}((0,0,0),(x_2,y_2,0)) = \sqrt{x_2^2 + y_2^2}$.

	$N = 1000$	$N = 2000$	$N = 4000$	$N = 6000$	$\mathbf{d}_{sR}(p_1,p_2)$
$x_2 = y_2 = \frac{1}{2}$	1.8628	0.8971	0.8655	0.7752	$\frac{\sqrt{2}}{2} \approx 0.7071$
$x_2 = y_2 = 1$	∞	1.9839	1.7267	1.5965	$\sqrt{2} \approx 1.4142$

Table 1. Mean distance $\mathbf{d}_{\mathrm{dsR}}((0,0,0),(x_2,y_2,0))$ for different N and sub-Riemannian distance, horizontal case.

If the number of vertices N is small, the graph Γ_r can be disconnected, in which case the distance between disconnected vertices is equal to infinity. In *Table 1* the value 0.8955 is the averaged distance of $\mathbf{d}_{\mathrm{dsR}}(p_1, p_2)$ calculated for 10 numerical experiments with 4000 random vertices each. As N increases, the dispersion of $\mathbf{d}_{dsR}(p_1, p_2)$ decreases and its value gets closer to the value of $\mathbf{d}_{sR}(p_1, p_2)$. The convergence of the distances in the vertical case is shown in *Table 2*.

	$N = 1000$	$N = 2000$	$N = 4000$	$N = 6000$	$\mathbf{d}_{sR}(p_1, p_2)$
$z_2 = \frac{1}{9}$	1.717	1.3617	1.2929	1.2702	$\frac{\sqrt{2\pi}}{3} \approx 0.8355$
$z_2 = \frac{4}{9}$	3.2894	2.8339	2.5877	2.5209	$\frac{2\sqrt{2\pi}}{3} \approx 1.671$

Table 2. Mean distance $\mathbf{d}_{\mathrm{dsR}}((0,0,0), (0,0,z_2))$ for different N and the sub-Riemannian distance, vertical case.

From Tables 1 and 2 one can see that, as N increases, the discrete sub-Riemannian distance gets closer to the standard sub-Riemannian distance in $\mathcal{H}$, but with different rates in the horizontal and vertical cases. A more detailed discussion on these results will be provided in the next section.

The last feature of geodesics in $\mathcal{H}$ that is going to be checked for Γ_r is the fact that the coordinate $z(t)$ of the geodesic that starts at O is proportional to the sectional area of the projection $(x(t), y(t))$ onto the Oxy plane. For the considered discrete model this projection is a polygon, see the upper right picture in Fig.4 The numerical experiment is the following:

1. Pick M test vertices p in Γ_r, whose third coordinate is $z(p)$;
2. Find the shortest path from O to p;
3. Calculate the polygon area $A(p)$ of the projected path.

For the Heisenberg group $z(p)$ and $A(p)$ are the same values, and, for example, the Dido's problem can easily be reformulated as a problem of finding geodesics [7]. The results for $\Gamma_{\frac{1}{2}}$ with $N = 3000$ random vertices and with $M = 200$ test vertices are presented in the Fig. 5. As the coordinate $z(p)$ is uniformly distributed in $[-1, 1]$, the dots with coordinates $(z(p), A(p))$ on Fig. 5 lie quite close to the plot of $|z(p)|$.

4. Tortuosity

First let us recall briefly what *tortuosity* is. Consider a domain $\Omega' \subset \mathbb{R}^3$ modeling a piece of porous media, such that there is a connected subset $P \subset \Omega'$ modeling the system of the media pores. Next, $\Omega' \setminus P$ simulates solid material. One can consider two arbitrary points $A, B \in P$ and the shortest path $\gamma(t)$, $t \in [0, 1]$ connecting A and B that fully lies in the system of pores P: $\forall t \in [0, 1]$ $\gamma(t) \in P$. The ratio of the length of γ and the
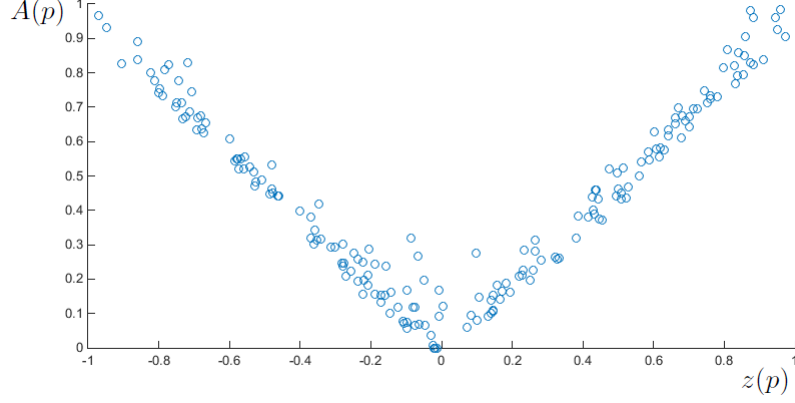
FIGURE 5. The coordinate $z(p)$ and the area $A(p)$ of the projected polygon for $M = 200$ test vertices in $\Gamma_{\frac{1}{2}}$.

standard Euclidean distance between A and B

$$\frac{\int\limits_0^1 |\dot{\gamma}(t)| dt}{\text{dist}_{Eucl}(A, B)}$$

called the *tortuosity τ of the path $\gamma(t)$.* If the media is homogeneous and isotropic and if $\text{dist}_{Eucl}(A, B)$ is sufficiently large, the tortuosity will be close to a limit value: it is greater than 1 and measures the level of entanglement of the system of pores. If the media is anisotropic then $\tau(A, B)$ will depend on the direction $\overrightarrow{AB}$.

Secondly, one can study the tortuosity of the Delaunay triangulation of uniformly distributed points [10]. It turns out that the ratio between the length $l_{triang}(A, B)$ of the shortest broken line connecting two points via edges of the triangulation and the Euclidean distance,

$$\frac{l_{triang}(A, B)}{\text{dist}_{Eucl}(A, B)},$$

converges from above to a fixed value $\tau_{Dln} \approx 1.05$ for a two-dimensional domain and $\tau_{Dln} \approx 1.09$ for a three-dimensional domain.

Next we come back to a domain Ω with the standard sub-Riemannian metric $\mathbf{d}_{sR}$ and the spatial graph Γ_r in Ω with vertices $p_i \in D$ and metric $\mathbf{d}_{dsR}$. The following ratio

$$\tau(A, B) = \frac{\mathbf{d}_{dsR}(A, B)}{\mathbf{d}_{sR}(A, B)} \tag{11}$$

is called the *tortuosity* of the path from A to B. This value depends on the set D of vertices, on the coordinates of B and on the parameter r of the graph Γ_r. It is a straight-forward generalization of the previously mentioned tortuosity.

Let us consider again two points $A = p_1$ and $B = p_2$ from the previous section. From Table 1, when both points lie in the horizontal plane $\{z = 0\}$ and the sub-Riemannian geodesic is a straight line, the tortuosity (11) gets close to τ_{Dln} in the three-dimensional case of the Delaunay tortuosity.

	$N = 1000$	$N = 2000$	$N = 4000$	$N = 6000$
$x_2 = y_2 = \frac{1}{2}$	2.6344	1.2687	1.2240	1.0963
$x_2 = y_2 = 1$	∞	1.4028	1.2210	1.1289

Table 3. The tortuosity $\tau((0,0,0),(x_2,y_2,0))$ for different N, horizontal case.

In the case of helicoidal geodesic, the difference between the sub-Riemannian and discrete sub-Riemannian distances becomes more evident:

	$N = 1000$	$N = 2000$	$N = 4000$	$N = 6000$
$z_2 = \frac{1}{9}$	2.0551	1.6298	1.5475	1.5203
$z_2 = \frac{4}{9}$	1.9685	1.6959	1.5486	1.5086

Table 4. The tortuosity $\tau((0,0,0),(0,0,z_2))$ for different N, vertical case.

Considering this 'anisotropic' behaviour of $\tau(A, B)$ we formulate the following

Conjecture on the limit tortuosity. *Consider a cubic domain $\Omega \subset \mathcal{H}$ with the sub-Riemannian distance $\mathbf{d}_{\mathrm{sR}}$ and the corresponding spatial graph Γ_r with N uniformly distributed vertices D and the discrete sub-Riemannian distance $\mathbf{d}_{\mathrm{dsR}}$. Fix two points $A = (0,0,0) \in D$ and $B = (\cos\varphi, 0, \sin\varphi) \in D$. As $N \to \infty$ one can choose a parameter of the graph Γ_r with the asymptotic*

$$r \sim c \cdot N^{-d} \text{ for some } c > 0, \ d > 0, \tag{12}$$

such that the tortuosity $\tau(A, B)$ converges to a limit tortuosity $\tilde{\tau} = \tilde{\tau}(\varphi)$ depending only on the coordinate φ of B for almost all positions of vertices in D. The limit tortuosity should be bounded

$$1 < \tilde{\tau} < C \ \forall \varphi \in [0, 2\pi].$$

Due to the fact that all considered functions are random variables the convergence of the tortuosity in this conjecture should be almost sure convergence. Finding optimal bounds for the constants c, d and C is another problem to consider. Also, the connection between d and the dimension (topological or Hausdorf) of the Heisenberg group is not clear.

We will say that a broken line with vertices $A = p_{i_1}, p_{i_2}, \dots, p_{i_k} = B$ is ε-close to a geodesic $\gamma(t)$, $t \in [t_0, t_1]$, connecting A and B if there is a

cylindrical neighbourhood of $\gamma(t)$

$$Cyl_\varepsilon = \bigcup_{t \in [t_0, t_1]} \{\gamma(t) + v | \forall v \in \mathbb{R}^3, \ |v| \le \varepsilon\},$$

containing all vertices p_i and all edges $[p_{i_j}, p_{i_j+1}]$ of the broken line.

Finally, we can formulate the approximation conjecture:

Approximation Conjecture. *Consider a cubic domain $\Omega \subset \mathcal{H}$ with the sub-Riemannian distance $\mathbf{d}_{\mathrm{sR}}$, the orresponding spatial graph Γ_r with N uniformly distributed vertices D and the discrete sub-Riemannian distance $\mathbf{d}_{\mathrm{dsR}}$. Fix two points $A = O \in D$ and arbitrary $B \in D$ and a sub-Riemannian geodesic $\gamma(t)$ connecting $A = \gamma(t_0)$ and $B = \gamma(t_1)$. For any ϵ there is number N of vertices and a parameter r satisfying (12) such that there is a shortest path $A = p_{i_1}, p_{i_2}, \ldots, p_{i_k} = B$ in the graph Γ_r which is ε-close to $\gamma(t)$.*

Note that if the point B lies on the Oz axis then there is no uniqueness of the sub-Riemannian geodesic connecting $A = O$ and B, it is defined up to rotation as it was mentioned earlier. In this case in the approximate conjecture one should choose an appropriate geodesic. It seems to be clear how to prove that in a cylindric neighbourhood of the fixed geodesic there is a broken line with vertices and edges from Γ_r. But how to prove that this broken line will be globally shortest path in Γ_r?

5. Conclusion.

Here we presented a discrete model Γ_r of the Heisenberg group $\mathcal{H}$ as a spatial graph with weighted edges. The weight of the edge is defined by the local sub-Riemannian distance $\mathbf{d}_{lsR}$, generated by the non-integrable Heisenberg distribution (1). The discrete sub-Riemannian distance $\mathbf{d}_{dsR}$ is the length of a shortest path in Γ_r. Numerical experiments give a motivation to formulate an approximation conjecture stating that shortest paths in the graph Γ_r will be sufficiently close to the geodesics in $\mathcal{H}$ if the number of vertices N is large enough and the parameter r is appropriately small.

The constructed model can be considered as a 'triangulation of the sub-Riemannian Heisenberg group', but without triangles. The triangulation of a smooth two-dimensional surface embedded in $\mathbb{R}^3$ is a collection of vertices, edges and triangles. In the non-integrable case there is no surface, so there should be no triangles. It is natural to choose a spatial graph Γ_r, consisting only of vertices and edges, as a model for non-integrable geometry.

We believe that the presented construction will be interesting both for specialists in discrete geometry and in sub-Riemannian geometry. The presented model can be useful for simulations of various processes in anisotropic medias, such as heat propagation, diffusion in anisotropic porous materials, deformations of layered solids, etc.

References

[1] E. Malkovich. On discrete sub-Riemannian geometry. International Conference on Geometric Analysis, 2022, p.82.

[2] J.E. Marsden, M. West. Discrete mechanics and variational integrators. Acta Numerica, 2001, 357-514.

[3] A.A. Simoes, J.C. Marrero, D.M. de Diego. Exact discrete Lagrangian mechanics for nonholonomic mechanics. Numerische Mathematik, Vol. 151, p. 49-98, 2022.

[4] Yu.N. Fedorov, D.V. Zenkov. Discrete nonholonomic LL systems on Lie groups. Nonlinearity 18(2005), 2211-2241.

[5] P.Popescu, M. Popescu. On discrete geometry of non-holonomic spaces. Proceedings of The International Conference "Differential Geometry and Dynamical Systems" (DGDS-2014), 1-4 September 2014, Mangalia, ROMANIA, BSG PROCEEDINGS 22 (2015) 69-74.

[6] V.N. Berestovskii, I.A. Zubareva. Shapes of spheres of special nonholonomic left-invariant intrinsic metrics on some Lie groups. Siberian Math. J.42(2001), no.4, 613–628.

[7] Yu. Sachkov. Introduction to Geometric Control. Springer Nature, 2022.

[8] E.W. Dijkstra. A note on two problems in connexion with graphs. Numerische Mathematik. (1959), 1: 269–271.

[9] V.N. Berestovskii. Geodesics of nonholonomic left-invariant intrinsic metrics on the Heisenberg group and isoperimetric curves on the Minkowski plane. Siberian Math. J., 35:1 (1994), 1–8.

[10] A.A. Bystrov, E.G. Malkovich. Tortuosity of Delaunay Triangulations and Statistics of Shortest Paths. Experimental Mathematics, 2024, October, 1–7. doi:10.1080/10586458.2024.2410189.